A Tandem Time--of--Flight Spectrometer for Negative--Ion/Positive--Ion Coincidence Measurements with Soft X-ray Excitation

Stråhlman, Christian; Sankari, Rami; Kivimäki, Antti; Richter, Robert; Coreno, Marcello; Nyholm, Ralf

Published in:
Review of Scientific Instruments

DOI:
10.1063/1.4940425

2016

REVIEW OF SCIENTIFIC INSTRUMENTS **87**, 013109 (2016)

A tandem time–of–flight spectrometer for negative–ion/positive–ion coincidence measurements with soft x-ray excitation

Christian Stråhlman,[1,a)] Rami Sankari,[1] Antti Kivimäki,[2] Robert Richter,[3] Marcello Coreno,[4] and Ralf Nyholm[1]

[1]*MAX IV Laboratory, Lund University, P.O. Box 118, 22100 Lund, Sweden*
[2]*Consiglio Nazionale delle Ricerche—Istituto Officina dei Materiali, Laboratorio TASC, 34149 Trieste, Italy*
[3]*Elettra–Sincrotrone Trieste, Area Science Park, 34149 Trieste, Italy*
[4]*Consiglio Nazionale delle Ricerche—Istituto di Struttura della Materia, 34149 Trieste, Italy*

(Received 23 October 2015; accepted 11 January 2016; published online 27 January 2016)

We present a newly constructed spectrometer for negative–ion/positive–ion coincidence spectroscopy of gaseous samples. The instrument consists of two time–of–flight ion spectrometers and a magnetic momentum filter for deflection of electrons. The instrument can measure double and triple coincidences between mass–resolved negative and positive ions with high detection efficiency. First results include identification of several negative–ion/positive–ion coincidence channels following inner-shell photoexcitation of sulfur hexafluoride (SF_6). © *2016 AIP Publishing LLC.* [http://dx.doi.org/10.1063/1.4940425]

I. INTRODUCTION

Studying photoinduced dissociation of molecules is of fundamental importance to chemical physics and the understanding of chemical bonds. Photoexcitation of molecules can induce a multitude of chemical processes, some of which lead to the fragmentation of the molecule. Under some circumstances, photoinduced fragmentation produces negative ions together with positive ions. Detecting and analyzing negative ions are not qualitatively different from positive ions; the same instruments can often be employed for both. Quadrupole mass filters,[1,2] time-of-flight (TOF) based instruments[3,4] and velocity map imaging (VMI)[5] have been used to measure negative-ion yields. The very same methods have been employed also in a few studies of negative and positive ions in coincidence, with TOF[6–9] and VMI[10–12] as the dominating techniques. Both approaches separate positive and negative particles by an electric field and accelerate them towards the respective detectors.

Negative–ion production from photoexcitation has received much less attention than that of positive ions. This is natural since negative–ion yields (NIY) are generally much smaller than positive–ion yields (PIY). This has to be compensated for by an increase of the transmission of the instrument and by increasing the intensity of the excitation, the latter being achievable with modern synchrotron radiation facilities. In addition, the instrument must effectively suppress the unwanted detection of electrons, which in an electrostatic instrument will follow the same paths as negative ions. An early version of an electron–deflecting filter by Schermann *et al.*[13] consisted of a small dipole electromagnet in a μ-metal casing. Since electrons are very light particles with small momenta, they are quite easy to deflect. TOF–based negative–ion spectrometers have used similar solutions either with permanent magnets or electromagnets.[8–10]

Negative–ion/positive–ion coincidences (NIPICO) have mostly been studied in small molecules with VUV and/or visible light using both laboratory and accelerator based sources.[6–8,10–12] NIPICO investigations have rarely exploited x-ray radiation; we are only aware of one study. Rühl and Flesch[9] observed double and triple coincidences at the C $1s \rightarrow \pi^*$ excitation in the CO_2 molecule using an instrument with two identical TOF spectrometers. Extending the analysis to multiple coincidences between the fragments (NIPIPICO: negative–ion/positive–ion/positive–ion coincidence) allowed them to study the kinetic energy release and chart the complete fragmentation path of the molecule. Their instrument could distinguish between different positive ions in coincidence with negative ions; however, the CO_2 molecule only produce one negative ion species.

We have designed a new instrument for detecting mass–resolved negative ions in coincidence with one or several mass–resolved positive ions. The instrument can identify NIPICO and NIPIPICO channels for samples where several species of negative ions are produced. It applies the TOF–based coincidence technique, with two spectrometers working in tandem, and a momentum filter for negative particles. The negative–ion spectrometer is specifically optimised for high transmission, which increases detection efficiency for coincidences. While the main goal of current experiments is the study of core–excited states in small molecules induced by soft x-ray excitation, the instrument could equally well be used for studies of valence–excited states.

This paper describes the instrument and discusses our design considerations. Acquisition modes for coincidence and calibration measurements are presented. We demonstrate detection and assignment of double and triple coincidences with high reliability and efficiency. In particular, the continuous acquisition of detector signals, with the instrument working with a constant extraction field, increases the efficiency of the instrumental setup. The performance of the instrument is demonstrated with a study on sulfur hexafluoride (SF_6),

a)Electronic mail: Christian.Strahlman@maxlab.lu.se

which is known to produce negative ions at the S 2p and F 1s edges.[14,15]

II. INSTRUMENT DESIGN

The setup consists of two time–of–flight ion spectrometers mounted facing each other. Both spectrometers operate under Wiley–McLaren focusing conditions[17] and share a 15 mm wide interaction region. The synchrotron light beam passes through the center of the interaction region where it crosses an effusive gas jet, which is let into the vacuum chamber through a gas needle perpendicular to the spectrometers and the light beam. An electric field in the extraction region separates positive and negative particles and accelerates them into the two spectrometers. The spectrometers are mounted at 54.7° (so called magic angle) relative to the polarization vector of the horizontally polarized light beam.

The spectrometer used for positive–ion detection was originally developed for a photoelectron/positive–ion coincidence (PEPICO) setup used at the Elettra storage ring and has been previously described in Ref. 18. The instrument consists of a 319 mm long and 40 mm wide stainless steel drift tube, preceded by two mesh holders, which create a 5 mm wide acceleration region and a 15 mm wide interaction region. Ions are detected by a Z-stacked triple MCP detector at the end of the drift tube. The tube and mesh holders are mounted on four steel rods, electrically isolated by PEEK spacers.

The negative–ion spectrometer was specifically designed to operate together with the existing positive–ion spectrometer without any changes to the latter. A second requirement was that an existing chamber be used, which put limits on the width and length of the instrument. In addition, we wanted to be able to use the new spectrometer as a stand–alone instrument, or in a PEPICO setup. To accommodate these needs, we have constructed the spectrometer with two interchangeable front parts, with and without an interaction region. In the NIPICO version, the original extraction region of the positive–ion spectrometer is used. The drift tube of the negative–ion spectrometer is docked to the grounded rods using four PEEK holders (see Fig. 1). The 5 mm long region created between the outer mesh of the interaction region and the outer drift tube mesh on the negative–ion spectrometer thus becomes the acceleration region for the negative–ion spectrometer. In the non-coincident version of the instrument, the PEEK spacers are interchanged with a complete extraction region including two holders with gold meshes (see Fig. 2).

As noted in Sec. I, the extraction of negative particles causes both negative ions and electrons to enter the negative–ion spectrometer. Since the number of electrons greatly outweighs that of the negative ions, they have to be deflected as not to saturate the detector and to improve the signal–to–noise ratio in coincidence experiments. This is most easily performed with a weak magnetic field in the drift tube. Simulations show that a magnetic field amounting to 15 G can deflect electrons with kinetic energies up to 3000 eV (electrons' high kinetic energies result from the acceleration into the drift tube), while the impact on flight paths, and associated flight times even of the lightest ions is negligible. We decided to generate the magnetic field from outside of the vacuum by mounting two small neodymium magnets on an adjustable holder on the vacuum chamber.

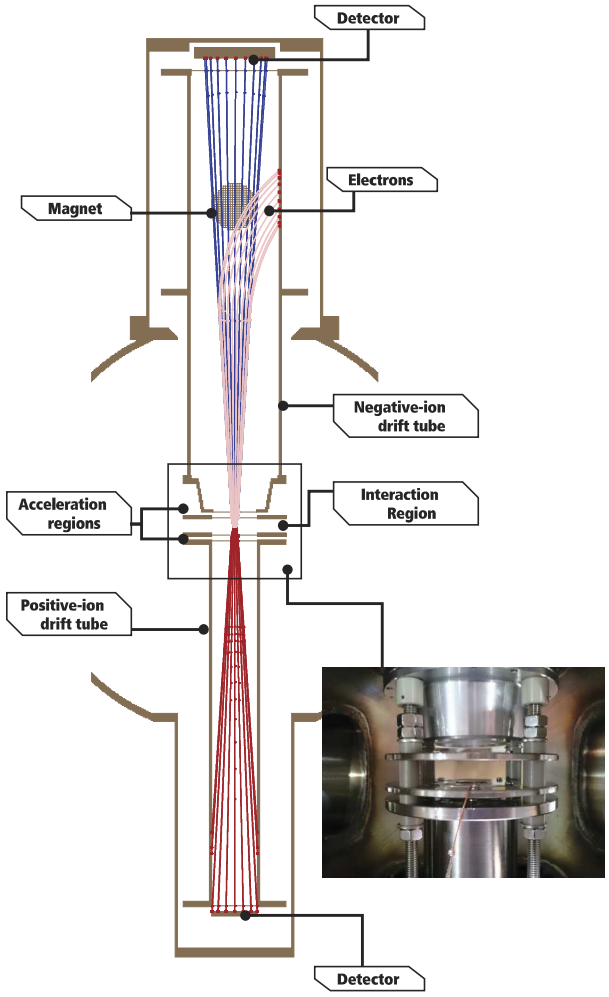

FIG. 1. Schematic drawing of the instrument setup with the negative–ion (top) and positive–ion (bottom) spectrometer. Negative ions, positive ions, and electrons are created in the interaction region and accelerated into the spectrometers. The inset depicts the interaction and acceleration regions (without needle) for the mounted spectrometer. Electrons are deflected in the negative–ion spectrometer by a weak magnetic field, provided by two small magnets outside vacuum (see also Fig. 2). The simulation shows trajectories of H^- ions (blue), H^+ ions (red) and electrons, each with 10 eV initial kinetic energy. The 15 G magnetic field only marginally deflects even the lightest ions. The positive–ion spectrometer is narrower and collects fast ion less efficiently. Simulations were performed with the SIMION software.[16]

The drift tube was made from an aluminum tube perforated by many small holes, 4 mm in diameter. The rationale behind this design is to minimize possible effects caused by secondary electrons created when deflected electrons with energies in the keV–range hit the inside of the drift tube. By using a perforated tube, the majority of electrons leaves the tube and becomes decelerated by the potential difference between the drift tube and the grounded vacuum chamber wall.

Since NIYs are small, a high transmission in the instrument is required. Light ions, particularly hydrogen ions (H^-), often escape detection in narrow TOF instruments since they tend to have high kinetic energies. A wider drift tube and larger detector area give a better collection efficiency even for

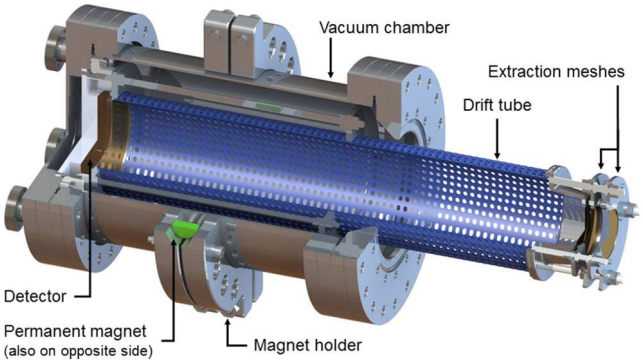

FIG. 2. Drawing of the negative–ion spectrometer in its stand-alone configuration with a separate interaction region. The magnetic field is provided by two external permanent magnets fixed by the movable magnet holder.

light ions. The detector for the negative–ion spectrometer is a commercial Hamamatsu double MCP with a circular, 77 mm in diameter, active area, and a single anode readout. Response time is 2 ns as stated by the manufacturer. Due to the detector design, the potential on the anode could not exceed +2800 V, referenced to ground potential. To achieve a suitable gain over the MCP stack, while avoiding a deceleration field between the MCP front and the drift tube end, the MCP front potential was limited to only +900 V. This defined the upper limit for the negative–ion spectrometer drift tube potential. In the experiments presented in this paper, the following potentials were used: extractor meshes ±92 V, negative–ion drift tube +854 V, positive–ion drift tube −740 V. In present settings, simulations performed with the SIMION software[16] showed that the negative–ion spectrometer accepts H^- ions with initial velocities perpendicular to the spectrometer axis corresponding to kinetic energies up to 5 eV. However, in the present coincidence setup, the total transmission is limited by the narrower positive–ion spectrometer.

The output pulses from the detectors were amplified and, after passing through a discriminator, read by a time-to-digital converter (TDC, model AM-GPX, manufactured by ACAM Messelectronic) with 80 ps time resolution. This system has been described in Ref. 18. The intensity of the light reaching the sample was monitored using a photodiode at the downstream exit of the chamber.

III. EXPERIMENTAL

The experiments were performed at the Gas Phase Photoemission beamline of the Elettra synchrotron radiation laboratory (Trieste, Italy). The beamline has been described in detail before.[19,20] Briefly, it uses an undulator as a light source and a spherical grating monochromator for the selection of the photon energy. The photon energy range of the beamline is 13.5–900 eV. High resolving power ($>10^4$) can be achieved at most energies thanks to five interchangeable gratings.

The light beam was centered in the interaction region by moving the frame of the spectrometer chamber. The effusive gas jet is let into the chamber through a gas needle controlled by a leak valve. The position of the needle was adjusted so that the photon beam crossed the gas jet in the interaction region. When the gas was introduced to the chamber, the pressure increased from the 3×10^{-8} mbar base pressure to 5×10^{-7} mbar, but it was estimated to be 10–50 times higher in the interaction region.

Having the permanent magnets mounted outside vacuum allowed us to quickly remove the magnetic field for testing the spectrometer performance. The position of the permanent magnets was optimized in several steps. Electrostatic simulations showed that there is a non-negligible probability that deflected electrons are focused back into the perforated drift tube and subsequently hit the detector. We indeed observed that some electrons were recorded in all acquisitions even after optimization. After optimizing the magnet positions in order to minimize the electron signal, we switched the polarity of the negative–ion spectrometer to measure positive ions instead. We could see that the measured flight times for ions matched simulations. We found that we had the most efficient reduction of electron signal when the magnets were positioned very close to the interaction region.

IV. PERFORMANCE AND FIRST RESULTS

To demonstrate the capabilities of the spectrometer and the NIPICO and NIPIPICO analysis, we have performed measurements of the SF_6 molecule. SF_6 is a well-known sample, and its photoexcitation properties have been investigated in several studies. NIYs and PIYs from photo-exited SF_6 have been measured in the inner-valence,[14] S 2p,[14,15] and F 1s regions.[15] The S 2p excitation spectrum of SF_6 displays several strong absorption resonances. The $6a_{1g}$ resonance lies below the 2p ionization threshold, while two shape resonances ($2t_{2g}$ and $4e_g$) are present above the ionization potential.[21] Several negative (and positive) ion channels have been identified. The molecule is therefore well suited for instrument testing.

The instrument can be operated in two different acquisition modes, where the first mode is aimed at flight time calibration and acquisition of mass resolved PIY and NIY, while the second is aimed at NIPICO and NIPIPICO analysis.

Calibration is performed in the pulsed extraction mode. An extraction field is produced by a pulsed high-voltage supply. We used an instrument from Directed Energy, Inc., model PVM 4210, controlled by a pulse generator (Stanford Research DG535) to produce two identical square pulses of opposite polarity with 92 V amplitude, 22 μs length, and 10 kHz repetition rate. The amplitude is determined by the Wiley–McLaren space focusing conditions.[17] The pulse trigger signal is used as the start trigger for the TOF measurement. This mode produces positive and negative TOF spectra independently and can therefore be used to measure the flight times of individual fragments. We measured positive–ion mass spectra with both spectrometers. The positive–ion spectrum measured by the negative–ion spectrometer was acquired by changing the polarity of all electrostatic potentials. The flight times of positive ions are identical to those of negative ions for opposite polarities. All measured flight times have an excellent match with SIMION simulations.

While it is in principle possible to deduce NIPICO events from the pulsed mode, in practice, the efficiency of the instrument is too low for this to be a feasible method. Because

the pulse is not correlated to the ionization process, many ions, even with low kinetic energies, have sufficient time to escape the interaction region before the pulse is applied. The pulsed operation therefore favors the detection of slow and heavy ions. In addition, due to the movements of the ions, the effective source size seen by the spectrometer spans the whole 15 mm wide interaction region. This causes a significant broadening of mass peaks (several 100 ns) compared to a PEPICO measurement where the ion is extracted almost immediately following its creation. This is particularly true with the present low-voltage settings.

The efficiency of the instrument is significantly increased by continuous extraction of positive and negative ions. Static electric fields are used to extract ions from the interaction region. Flight–time differences of two fragments can be constructed from the hits of ions on the two detectors. Combined with flight times measured in the pulsed mode and aided by simulations of flight times for all possible negative and positive ionic fragments, each flight–time difference can be assigned to a coincidence between a specific negative ion and a specific positive ion.

Signals can be recorded in two ways. In the first analysis scheme (*negative ion trigger*), a detection of a negative ion provides a start signal for the timing electronics, while a subsequent detection of a positive ion gives a stop. The positive–ion signal is delayed electronically to ensure that it arrives after the corresponding start signal. (Typically the delay should be slightly larger than the difference between expected flight times of the slowest negative ion and the fastest positive ion.) While this scheme is the most efficient way to record coincidences between two fragments (NIPICO) the detection of three or more coincident fragments is inhibited. The second analysis scheme (*continuous trigger*) records all hits at both detectors continuously. The coincidence events are established afterwards in the computer analysis. In principle, coincidences between several negative and several positive fragments can be recorded. In our analysis, we have restricted ourselves to coincidences between one negative and (up to) three positive fragments.

NIPICO spectra were measured with negative ion triggering at the main resonances in the S 2p region. Each acquisition lasted 120 min and the positive ions were recorded with a 8000 ns delay. Fig. 3 shows complete TOF spectra acquired at four photon energies. The spectra display a multitude of peaks and features among which only few are true NIPICO events. Positions for the main coincidence channels are indicated. These peaks have been identified to be true NIPICO peaks by comparing with spectra where the drift tube potential on the negative–ion spectrometer was increased by 45 V. The measured TOFs of NIPICO peaks are expected to shift towards longer times, while PEPICO peaks should not display any significant shift. Only the indicated NIPICO peaks, corresponding to SF^-/F^+, S^-/F^+, F^-/F^+, and F^-/S^+ coincidences, did shift. The S^-/F^+ and F^-/F^+ peaks show a pronounced splitting due to kinetic energy release in the fragmentation. Towards longer flight times, several PEPICO channels are present. These arise from electrons which are not completely removed by the deflection in the negative–ion spectrometer. Their expected positions can be simulated and can serve as calibration peaks since all pairs of PEPICO and NIPICO peaks with identical positive ion participants should be equally distanced from each other.

The sharp peak at $t = 0$ marks events where the two detectors recorded hits almost simultaneously. The probable explanation for these events is spurious crosstalk between the two detectors, possibly caused by the power supply. Due to hardware errors in the TDC card, additional sharp features can be seen in the spectra—both positive peaks (e.g., the large peak at −1100 ns and several smaller peaks below −4000 ns) and negative peaks (at −3000 ns and repeated every 5000 ns). These are not related to any true process, as verified by comparing spectra recorded with slightly increased drift tube potentials of the two spectrometers, one at a time. Only true NIPICO and PEPICO peaks were observed to shift their

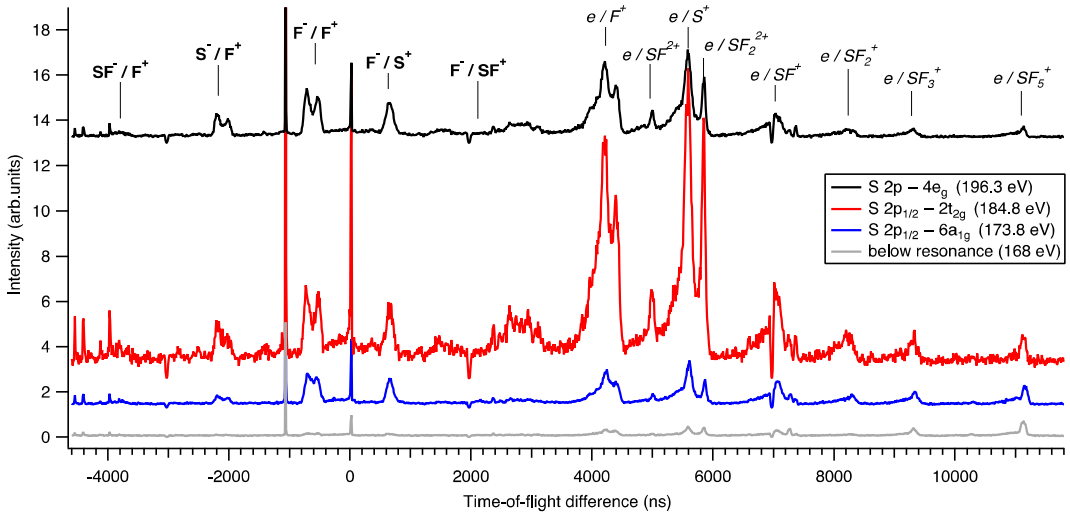

FIG. 3. Complete NIPICO spectra for three resonances in the S 2p region of SF_6 (black, red, and blue), together with a reference spectrum below resonances (gray). Each spectrum was acquired for 120 min. The intensity has been normalized to the beam intensity, as measured by the photodiode. Five NIPICO channels have been marked. All peaks in the 3500–12 000 ns region belong to the PEPICO spectrum created from residual electrons in the negative–ion spectrometer. The origin of other false peaks is discussed in the text.

positions in accordance with calculated flight times for the increased potentials. The two broad features at 1500 ns and 2700 ns cannot be assigned to any PEPICO channel, but they appear to shift when changing the drift tube potential of the positive–ion spectrometer. It is plausible that these features arise from the detection of secondary electrons in coincidence with positive ions. Their positions match coincidences triggered from electrons that are created when positive ions hit meshes in the positive–ion spectrometer during flight.

Core–excited states predominantly decay by emission of Auger electrons. Thus, a fragmentation process including one negative ion is likely to produce several positive ions. Fig. 4 shows the results from a continuous trigger measurement at the F 1s $\rightarrow 6t_{1u}$ excitation ($h\nu$ = 693.5 eV). From the map we can identify four triple–coincidence channels involving one negative and two positive fragments. It should be noted that the $F^-/SF^+/F^+$ channel is clearly visible in the NIPIPICO map, while the F^-/SF^+ channel hardly shows up in the NIPICO spectrum. This is indeed expected since the detection of a fast F^+ fragment in the negative ion trigger scheme inhibits the subsequent detection of a slower SF^+ fragment. While our instrument is capable of measuring even higher order coincidence channels, such as NIPIPIPICO, no such events could be identified in the current dataset.

Some general observations can be made regarding the acquisition modes. In the continuous extraction mode, the identity of the complete negative–ion/positive–ion pairs is determined by the flight–time difference of the two fragments. In simple molecules with few possible fragments this is straightforward since the possible combinations of positive and negative ions are few. In more complicated molecules, such as SF_6, there are more combinations, and also an increasing risk for a temporal overlap between several pairs. In addition, since electron counts cannot be completely avoided, there is also a risk of a temporal overlap between electron/positive–ion and negative–ion/positive–ion coincidences. To avoid temporal overlaps between these processes, we have used simulations to adapt the flight times of all possible ion and electron combinations in order to find a combination of voltages that produces no overlaps. In the case of SF_6, only pairs of the lightest negative ions in coincidence with the heaviest positive ions overlap in part with electron/medium-heavy–positive–ion coincidences. For a definite measurement of these channels, pulsed mode coincidence measurements has to be performed. As the expected yield of these coincidences is very low, we have not performed such time–consuming measurements.

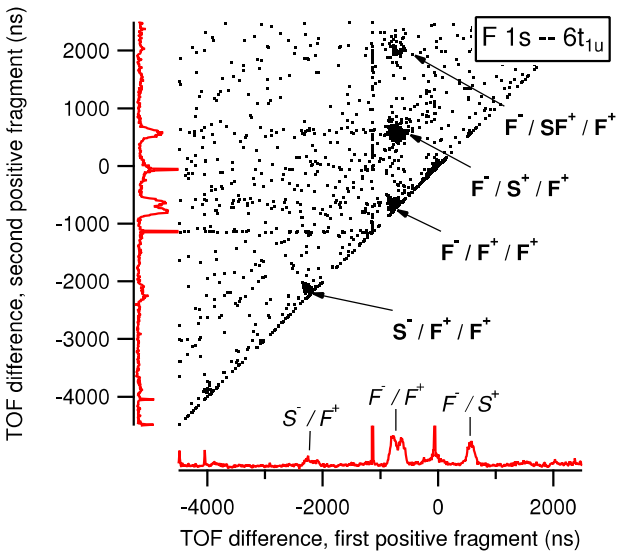

FIG. 4. NIPIPICO map measured at the F 1s $\rightarrow 6t_{1u}$ excitation ($h\nu$ = 693.5 eV) of SF_6. The map was acquired during 60 min. The bottom axis displays the time–of–flight difference between the first positive fragment and the negative fragment (as in Fig. 3), while the left axis shows the time-of-flight difference between the second positive fragment and the (same) negative fragment. The map thus shows the triple–coincidence between one negative and two positive fragments. Four triple–coincidence channels can be identified in this map. The increased yield at $t_1 = 0/t_2 = 0$ can be attributed to spurious crosstalk between detectors (see text).

V. DISCUSSION

In this section, we briefly discuss scientific results that can be extracted from the presented data. While a complete analysis is beyond the scope of this paper, some initial results are outlined in order to illustrate the capabilities of the technique. While new insights into the negative ion formation from SF_6 can be extracted from the NIPICO data, a more comprehensive analysis of the dissociation pathways would greatly benefit from complete NIPIPICO yields. Additional such data at the S 2p edge will be collected in subsequent experiments.

Our NIPICO measurements (Fig. 3) show three clear coincidence channels, S^-/F^+, F^-/F^+, and F^-/S^+, at all three resonances. Their relative intensities can be compared to the valence–subtracted photoionization cross sections at these resonances. We estimate from the data of Ref. 22 that ionization at the S $2p_{1/2} \rightarrow 2t_{2g}$ shape resonance occurs with ~3.5 times higher probability than at the S $2p_{1/2} \rightarrow 6a_{1g}$ excitation and with ~2.3 times higher probability than at S $2p \rightarrow 4e_g$ shape resonance. When compared to ionization cross sections, we observe higher relative yields of F^-/F^+ and F^-/S^+ coincidences at the $6a_{1g}$ excitation than at the $2t_{2g}$ shape resonance. The $2t_{2g}$ shape resonance represents a temporary trapping of the S $2p$ photoelectron by a barrier in the molecular potential,[23] after which it is considered to decay so that the trapped electron tunnels into the continuum. The result is a S $2p$ ionized state, which typically decays via Auger transitions to doubly charged final states. Instead, at the S $2p_{1/2} \rightarrow 6a_{1g}$ excitation, the core-excited state is neutral and the final states after decay via electron emission (resonant Auger decay) are mostly singly ionized valence–excited states. Our coincidence spectra therefore show that the production of F^-/F^+ and F^-/S^+ ion pairs is more likely after core excitation than core ionization. The trend is understandable, since negative ions could obviously be released more easily if dissociating valence states after (resonant) Auger decay are less positively charged.

We also observe that all the negative-ion/positive-ion coincidence peaks are more intense at the $4e_g$ shape resonance than at the S $2p_{1/2} \rightarrow 2t_{2g}$ shape resonance, when normalized to the photoionization cross section. This can be explained by the multielectron character of the $4e_g$ shape resonance. Ferrett *et al.*[23] observed that a shake-up satellite of the S $2p$ photoelectron line is hugely enhanced at the $4e_g$ shape

resonance, gaining an intensity of even 30% of those of the S $2p$ main lines. The electron configuration of the satellite is of type S $2p^{-1}val^{-1}virt^{1}$, where val is a valence orbital and $virt$ is an orbital that is unoccupied in the molecular ground state. When these core hole states decay via Auger transitions, they produce mostly excited states of the doubly charged parent ion, as the electron in the $virt$ orbital more likely acts as a spectator than participates in the decay. It is not yet known whether the presence of such an electron in the final states increases the production of negative ions or not. However, the S $2p$ shake-up states may also decay with small probability via S $2p$ fluorescence emission. This decay channel populates excited final states of the singly ionized molecule, similarly to resonant Auger decay at the S $2p_{1/2} \rightarrow 6a_{1g}$ excitation below the S $2p$ ionization potential. Radiative decay channel of the shake-up states is therefore expected to contribute to the production of negative ions. Also core-valence double excitations (to S $2p^{-1}val^{-1}virt^{1}_{1}virt^{1}_{2}$ core-excited states) may occur at the $4e_g$ shape resonance.[23] Their resonant Auger decay would also lead to excited states of the singly ionized molecular ion, and after dissociation reactions to negative ions. In summary, among multielectron transitions, both the S $2p$ shake-up ionization and core-valence double excitations can increase the production of negative ions.

While it has been suggested previously that NIY is a sensitive tool to assign above–threshold resonances in diatomic and triatomic molecules,[24] it is not the case for a larger molecule such as SF_6.[15] It has been argued that a larger molecular system is able to dissipate many positive charges over several smaller fragments. Indeed, the dominance of negative and positive F, S, and SF ions generally in the NIPICO and NIPIPICO spectra suggests that production of negative ions from core-excited SF_6 is a process where the molecule breaks into many small fragments. So far, none of our measured resonances at the S 2p or F 1s edge have displayed a coincidence channel involving any ionic fragment heavier than $SF^{\pm}$. NIY from valence excitation,[2] in contrast, has a significant contribution from the heavy SF_5^- fragment as well as the lighter F_2^-. This observation further strengthens the rationale for a complete NIPIPICO study to unfold the dissociation pathways in core-excited SF_6, including the contribution of radiative decay in negative ion production.

VI. CONCLUSIONS AND OUTLOOK

We have constructed and commissioned a new instrument to measure negative–ion/positive–ion coincidences from gas phase molecules. The instrument is able to measure coincidences between one negative and several positive fragments originating from a single fragmentation event. The instrument builds on well understood TOF techniques together with magnetic deflection of unwanted electrons. The NIPICO and NIPIPICO technique provides a tool to further increase the understanding of the molecular fragmentation process, particularly with the new abilities to study negative ion production.

We foresee some changes that will improve the performance of the instrument. Rebuilding the detector holder would allow us to run the negative–ion spectrometer in a larger range of acceleration potentials, thus avoiding temporal overlaps between coincidence channels. An increased MCP gain can also increase the detection efficiency for heavier ions. Increasing the drift tube potential also increases temporal resolution and transmission for high-energy ions. Second, the magnetic deflection needs to be improved in order to provide a more localized magnetic field in the drift tube. This is essential to properly steer the deflected electrons and further reduce electron counts on the negative–ion detector, thus increasing the purity of the spectra. A possible future development of the instrument to include position sensitive detectors for both negative and positive ions would increase the amount of information rendered from the experiment, especially to chart in more detail the dissociation dynamics in negative–ion producing channels. Further scientific studies on small organic molecules are planned for the coming year.

ACKNOWLEDGMENTS

The authors acknowledge E. S. El Afifi and the staff at the workshop at MAX IV Laboratory for their assistance with the design and production of the negative-ion spectrometer. We thank D. Benedetti (CNR–IOM) for assistance in designing the support for the TOF spectrometers as well as M. Barnaba and G. Bortoletto (Elettra–Sincrotrone Trieste) for the construction of new pieces for the support. J. Winqvist has assisted with graphical design of figures in this article. We acknowledge Elettra–Sincrotrone for providing beamtime (Proposal No. 20145053) and the staff at Elettra for their assistance during commissioning. The research leading to these results has received funding from the European Community's Seventh Framework Programme (FP7/2007-2013) under Grant Agreement No. 312284.

[1]K. Mitsuke, S. Suzuki, T. Imamura, and I. Koyano, J. Chem. Phys. **92**, 6556 (1990).
[2]M. J. Simpson and R. P. Tuckett, Int. Rev. Phys. Chem. **30**, 197 (2011).
[3]Q. Feng, S.-X. Tian, Y.-J. Zhao, F.-Y. Liu, X.-B. Shan, and L.-S. Sheng, Chin. Phys. Lett. **26**, 053402 (2009).
[4]E. Rühl and H.-W. Jochims, Z. Phys. Chem. **195**, 137 (1996).
[5]Y. Hikosaka and E. Shigemasa, J. Electron Spectrosc. Relat. Phenom. **148**, 5 (2005).
[6]K. Mitsuke, H. Yoshida, and H. Hattori, Z. Phys. D **27**, 267 (1993).
[7]H. Yoshida and K. Mitsuke, J. Electron Spectrosc. Relat. Phenom. **79**, 487 (1996).
[8]H. Yoshida and K. Mitsuke, J. Chem. Phys. **100**, 8817 (1994).
[9]E. Rühl and R. Flesch, J. Chem. Phys. **121**, 5322 (2004).
[10]Y. Hikosaka and J. H. D. Eland, Rapid Commun. Mass Spectrom. **14**, 2305 (2000).
[11]S. Marggi Poullain, K. Veyrinas, P. Billaud, M. Lebech, Y. J. Picard, R. R. Lucchese, and D. Dowek, J. Chem. Phys. **139**, 044311 (2013).
[12]C. Elkharrat, Y. J. Picard, P. Billaud, C. Cornaggia, D. Garzella, M. Perdrix, J. C. Houver, R. R. Lucchese, and D. Dowek, J. Phys. Chem. A **114**, 9902 (2010).
[13]C. Schermann, I. Cadez, P. Delon, M. Tronc, and R. I. Hall, J. Phys. E: Sci. Instrum. **11**, 746 (1978).
[14]S. W. J. Scully, R. A. Mackie, R. Browning, K. F. Dunn, and C. J. Latimer, J. Phys. B: At., Mol. Opt. Phys. **35**, 2703 (2002).
[15]M. N. Piancastelli, W. C. Stolte, R. Guillemin, A. Wolska, S.-W. Yu, M. M. Sant'Anna, and D. W. Lindle, J. Chem. Phys. **122**, 094312 (2005).
[16]See http://simion.com/ for SIMION.
[17]W. C. Wiley and I. H. McLaren, Rev. Sci. Instrum. **26**, 1150 (1955).
[18]O. Plekan, M. Coreno, V. Feyer, A. Moise, R. Richter, M. de Simone, R. Sankari, and K. C. Prince, Phys. Scr. **78**, 058105 (2008).

[19]R. Blyth, R. Delaunay, M. Zitnik, J. Krempasky, R. Krempaska, J. Slezak, K. Prince, R. Richter, M. Vondracek, R. Camilloni, L. Avaldi, M. Coreno, G. Stefani, C. Furlani, M. de Simone, S. Stranges, and M.-Y. Adam, J. Electron Spectrosc. Relat. Phenom. **101-103**, 959 (1999).
[20]K. C. Prince, R. R. Blyth, R. Delaunay, M. Zitnik, J. Krempasky, J. Slezak, R. Camilloni, L. Avaldi, M. Coreno, G. Stefani, C. Furlani, M. de Simone, and S. Stranges, J. Synchrotron Radiat. **5**, 565 (1998).
[21]E. Hudson, D. A. Shirley, M. Domke, G. Remmers, A. Puschmann, T. Mandel, C. Xue, and G. Kaindl, Phys. Rev. A **47**, 361 (1993).
[22]M. Stener, P. Bolognesi, M. Coreno, P. O'Keeffe, V. Feyer, G. Fronzoni, P. Decleva, L. Avaldi, and A. Kivimäki, J. Chem. Phys. **134**, 174311 (2011).
[23]T. A. Ferrett, D. W. Lindle, P. A. Heimann, M. N. Piancastelli, P. H. Kobrin, H. G. Kerkhoff, U. Becker, W. D. Brewer, and D. A. Shirley, J. Chem. Phys. **89**, 4726 (1988).
[24]W. C. Stolte, D. L. Hansen, M. N. Piancastelli, I. Dominguez Lopez, A. Rizvi, O. Hemmers, H. Wang, A. S. Schlachter, M. S. Lubell, and D. W. Lindle, Phys. Rev. Lett. **86**, 4504 (2001).